molecular pharmaceutics

Article

pubs.acs.org/molecularpharmaceutics

Avidity Mechanism of Dendrimer–Folic Acid Conjugates

Mallory A. van Dongen,[†] Justin E. Silpe,[‡] Casey A. Dougherty,[†] Ananda Kumar Kanduluru,[∥] Seok Ki Choi,[§] Bradford G. Orr,[⊥,§] Philip S. Low,[∥] and Mark M. Banaszak Holl*[,†,‡,§]

[†]Department of Chemistry and [⊥]Department of Physics, [‡]Program in Macromolecular Sciences and Engineering, and [§]Michigan Nanotechnology Institute for Medicine and Biological Sciences, University of Michigan, Ann Arbor, Michigan 48019, United States

[∥]Department of Chemistry, Purdue University, West Lafayette, Indiana 47907, United States

Supporting Information

ABSTRACT: Multivalent conjugation of folic acid has been employed to target cells overexpressing folate receptors. Such polymer conjugates have been previously demonstrated to have high avidity to folate binding protein. However, the lack of a monovalent folic acid–polymer material has prevented a full binding analysis of these conjugates, as multivalent binding mechanisms and polymer-mass mechanisms are convoluted in samples with broad distributions of folic acid-to-dendrimer ratios. In this work, the synthesis of a monovalent folic acid–dendrimer conjugate allowed the elucidation of the mechanism for increased binding between the folic acid–polymer conjugate and a folate binding protein surface. The increased avidity is due to a folate-keyed interaction between the dendrimer and protein surfaces that fits into the general framework of slow-onset, tight-binding mechanisms of ligand/protein interactions.

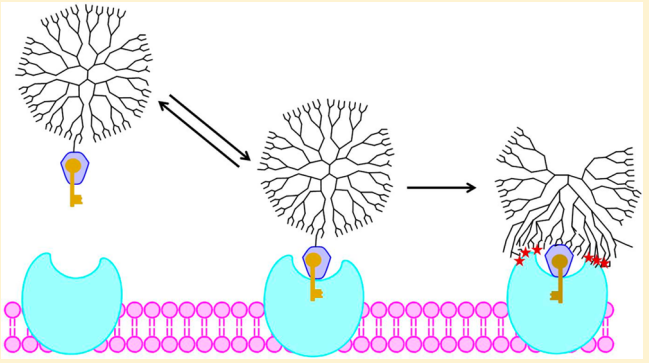

KEYWORDS: *PAMAM dendrimer, folic acid, multivalent binding, polymer/protein interactions*

INTRODUCTION

Folic acid (FA) targeting has been extensively studied for improving the therapeutic index of drugs.[1−6] Although the molecular-level structure of this interaction has only recently been fully elucidated,[7] substantial progress has still been made over the past 20 years in FA targeting, with seven drug conjugates advancing to clinical trials. Targeting of a drug or drug conjugate exploits the interaction of this vitamin with a high affinity ($K_d \sim 0.1$ nM)[2] folic acid receptor (FAR), which is overexpressed in many cancer cells. This receptor is also found in healthy epithelial cells; however, these are generally inaccessible to FA bearing conjugates in the blood,[2] enabling this system to exploit cytotoxic effects of drugs while minimizing collateral damage in healthy tissues. In addition to cell surface targeting, FA conjugation provides a selective uptake pathway for the conjugated drug via folate receptor mediated endocytosis and release of the FA/conjugate from the receptor and endosome.[8,9] Many targeted small molecule delivery designs take advantage of this highly specific interaction including examples such as doxorubicin,[10] methotrexate,[11] protein toxins,[12] imaging agents,[13,14] and immunotherapeutics[15] both *in vitro* and *in vivo* by exploiting carrier mechanisms including liposomes,[16] inorganic nanoparticles,[13] and organic polymers.[17−19]

Multivalent conjugates of ligands to nanomaterials are often employed purposefully to increase the avidity and/or specificity of an interaction or accidentally as a result of stochastic synthetic approaches. The enthalpic and entropic mechanisms through which multivalency increases the interaction of a ligand and its target have been extensively studied from a theoretical viewpoint.[20−24] Briefly, there are two main multivalent effects that may contribute to the system studied here; those dependent on the increased effective (or local) concentration, and those due to multiple binding events occurring for a single conjugate.[25] Higher local concentrations can result in higher affinities, and an increased chance of rebinding upon dissociation of the initial interaction ("statistical rebinding") or secondary binding events.[26,27] Multivalent classifications have been discussed and reviewed elsewhere by Kiessling,[28,29] Whitesides,[25] and Cloninger.[26]

Although multivalent conjugates of many dyes, drugs, and targeting ligands (including FA) have been developed, the actual impact of the specific number of ligands on improvements in avidity and/or biological activity has been difficult to analyze due to the heterogeneous mixtures generated by stochastic conjugation chemistries employed in their synthesis.[30] For example, a stochastic conjugation of 3 equiv of FA to a scaffold with multiple functionalizable sites (≥30) results in a sample with a mean of ∼3 FAs per scaffold, but also a

Received: January 31, 2014
Revised: March 18, 2014
Accepted: March 28, 2014
Published: April 11, 2014

distribution of unique conjugates with FA-to-scaffold ratios ranging from 0 to ∼11 FA molecules per scaffold (Figure 1).

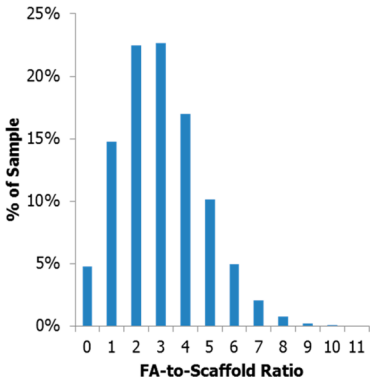

Figure 1. Distribution of conjugates resulting from a stochastic conjugation of 3 equiv of FA to 1 equiv of scaffold.

Previous efforts to quantify multivalent binding constants have employed surface plasmon resonance (SPR) to measure increases in binding between materials containing different average numbers of ligands (folic acid[31] and methotrexate[32−34]) and folate binding protein (FBP) modified surfaces. The binding constant of folic acid to FBP, K_d ∼ 5−10 μM, is roughly 1000-fold weaker than observed for folate receptor.[31,35] Although these studies have reported a general trend of greater avidity with increased valency, the utilization of materials containing a distribution of ligand-to-scaffold ratios complicated understanding the mechanisms involved in multivalent binding, or elucidation of the relative activity of the various components in the sample. For example, does the entire population illustrated in Figure 1 with two or more conjugated FAs (80% of the population) enable equivalent receptor clustering in a cell? Or does a higher valency, and consequently higher effective concentration, such as 5−11 FAs per scaffold (18% of the population) produce all of the observed activity?

Poly(amidoamine) (PAMAM) dendrimer is an extensively studied vector for the multivalent, targeted delivery of drugs, genes, and imaging agents.[36,37] The dendritic architecture has many advantages for biomedical applications, including low polydispersity, internal core space available for the entrapment of drugs, and multiple branches providing terminal groups for functionalization.[38] PAMAM dendrimer is particularly suited for such applications due to its protein-like architecture, low immunogenicity, ability to solubilize hydrophobic small molecules, and easily functionalized primary amine terminal surface groups.[39−41] The size of generation 5 (G5) PAMAM (5.4 nm diameter) is also ideal for vascular delivery and excretion due to kidney filtration.[42] Recent advancements have enabled the isolation of monomeric G5 PAMAM dendrimers from oligomeric (dimer, trimer, etc.) and trailing generation defects (G1−G4), narrowing the experimentally realized size distribution of this vector from 1−115 kDa (commercial material) to 25−29 kDa.[43] Possible convolution of results by large mass differences and vector-accessible surface area is eliminated by removing both trailing generations and oligomers from the G5 PAMAM monomer material.

In 2007, Banaszak Holl et al. employed SPR to measure the increased avidity to FBP and cellular uptake of G5 PAMAM−FA conjugates as a function of average number of attached FAs (Figure 2).[31] The dissociation constant (k_d) was observed to exponentially decrease as the average valency of FA increased; however, this calculation assumed that given a long enough experiment all bound materials would dissociate from the surface and that the experimental sensorgram would return to

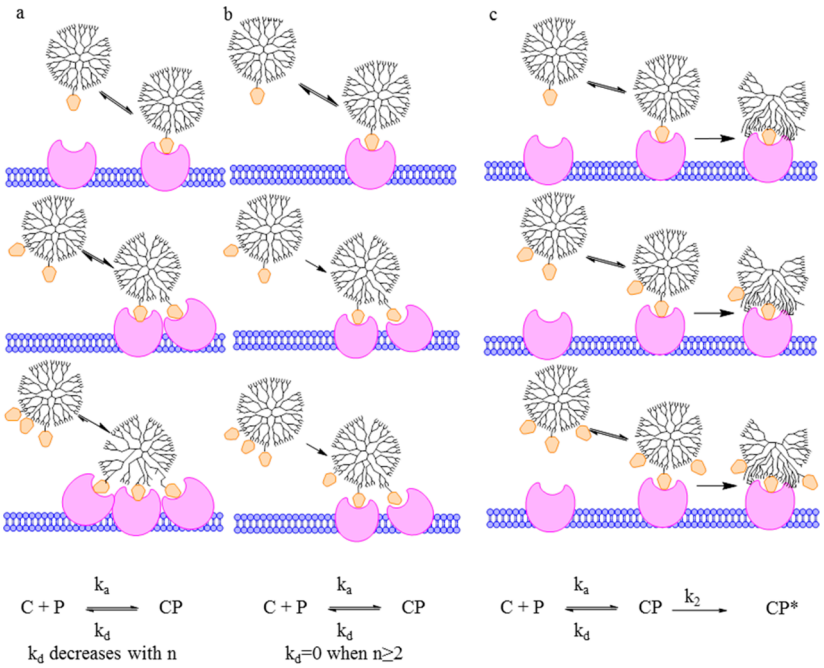

Figure 2. Proposed models for enhanced G5−FA binding to FBP. (a) Multivalent binding increases avidity with increasing valency. (b) Any multivalent binding (2 or more interactions) is irreversible, and monovalent binding is reversible. (c) FA "keys" the initial interaction between conjugate and FBP, which is followed by strong nonspecific interaction between the dendrimer and protein. C represents G5−FA_n conjugate, P is FBP, CP a complex between a conjugate and $n \geq 1$ FBP. CP* is a tight complex formed by a conformation change in the polymer and the resulting polymer−protein interaction.

dx.doi.org/10.1021/mp5000967 | *Mol. Pharmaceutics* 2014, 11, 1696−1706

the level of signal present prior to G5−$FA_{n(avg)}$ exposure. The nonlinear (exponential) behavior in k_d was attributed to a saturation of FA−FBP binding events limited by the immobilized protein density on the SPR flow cell surface and not to the valency of FA (Figure 2a). Interestingly, the same trend in signal saturation as a function of FA valency was observed for mean fluorescence, as measured by flow cytometry when equivalent conjugates labeled with a dye were evaluated for binding to FAR upregulated KB cells. This observation was interpreted as an indication that the dendrimer conjugates do not trigger receptor clustering on the cell surface, which would allow for higher affinities as more proteins became available.

Subsequent analyses of this data, employing different assumptions, resulted in two alternate mechanisms for explaining the changes in binding as a function of average valency. In 2010, Waddell, Sander et al. reanalyzed the original data set and proposed that the binding of the conjugates occurs via two distinct interactions.[44] This mechanism acknowledges the broad distribution of ligand-to-dendrimer ratios present in stochastically synthesized materials, including dendrimers that have zero FA, one FA, or two or more FAs. It was proposed that (1) monovalent interaction between G5−FA_1 and one FBP is attributable to binding that is reversible on the time scale of the experiment and (2) multivalent binding between G5−$FA_{\geq 2}$ to two or more FBPs is irreversible on the SPR experimental time scale (Figure 2b). Waddell, Sander, et al. hypothesized that the increased avidity attributed to valency increase by Banaszak Holl et al.[31] actually arises from decreased amounts of zero-functional and monofunctional conjugates in the stochastic average material. This mechanism still proposes that FA-based multivalent binding is important. The original flow cytometry data can be similarly interpreted; receptor clustering is achieved by bivalent conjugates, and further increasing of valency has no measurable effect on the cell. A very different mechanism based on kinetic limitations of cooperativity was proposed by Licata and Tkachenko in 2008.[45] This study concludes that the increased avidity proposed for the G5−$FA_{n(avg)}$ conjugates[31] is higher than can be attributed to cumulative effects of multivalent binding and that kinetic limitations actually prevent the type of multivalent interactions proposed in Figures 2a and 2b. They propose that the enhanced interaction observed by SPR is a result of van der Waals interactions between the polymer vector and protein/chip surface that are enabled by a single key−lock binding between FA and FBP (Figure 2c).

The broad distribution of folic acid-to-dendrimer ratios present in each sample, including both monovalent and multivalent conjugates in the low average materials, prevented a clear experimental elucidation between the three models depicted in Figure 2. In particular, a conjugate with a precise ratio of 1 FA per dendrimer (G5−FA_1) was lacking to determine if the observed increase in avidity was a product of multivalent binding between the conjugate and SPR surface (Banaszak Holl and Sander mechanisms)[31,44] or a single FA−FBP lock-and-key combined with van der Waals polymer/surface interaction (Licata and Tkachenko mechanism).[45]

In order to address these materials-based challenges to understanding multivalency, we have developed click chemistry and reverse-phase high performance liquid chromatography (rp-HPLC) methods to isolate dendrimers conjugated to precise numbers of ligands (i.e., G5-L_x, x = 0−4, where "x" is not a mean value).[30,46,47] These methodologies, which have been previously demonstrated to be successful for azide[30,46,48] and fluorinated, ring-strain-promoted click ligands,[48] are now extended to a second ring strain promoted ligand (cyclooct-1-yne-3-glycolic acid (COG)), which has been used in previous G5−$FA_{n(avg)}$ SPR studies.[33] In principle, isolating the precise ratio samples G5−FA_x, x = 1, 2, 3, etc., would allow SPR experiments where the multivalent binding effect is decoupled from the heterogeneity of stochastic samples (G5−$FA_{n(avg)}$). The isolated G5-L_x were "clicked" with a γ-azide-Lys-Asp-FA derivative (γ-azide-FA). The resulting samples include a G5-PAMAM dendrimer with a FA-to-dendrimer ratio of 0.96 that contains no detectable multivalent G5−$FA_{\geq 2}$ species: the sample needed to differentiate the three mechanistic hypotheses proposed to date. The remainder of the click reactions did not proceed with 100% efficiency, but still yielded samples that contained a well-defined high-n cutoff and had a narrower-than-stochastic distribution of FA-to-dendrimer ratios. The binding of these conjugates was analyzed by SPR on both high and low FBP density surfaces. The results indicate that, at either surface FBP density, total folic acid concentration is the dominant factor leading to increased amounts of bound material with increased valency. Only a small multivalent effect is observed for G5−$FA_{\geq 2}$ material because of increased statistical rebinding as compared to G5−FA_1. Most importantly, the G5−FA_1 sample exhibited the same irreversible binding to the FBP surface, on the SPR time scale, as the G5−$FA_{\geq 2}$ samples. This experimental result conclusively rules out the earlier mechanistic hypotheses by Banaszak Holl et al.[31] and by Sander et al.[44] and provides strong experimental support for the key−lock/van der Waals mechanism proposed by Licata and Tkachenko.[45] This mechanism falls into the general class of slow-onset, tight binding interactions[49,50] between ligand and protein albeit with the novel feature of polymer adsorption onto the protein surface to yield the final tight-binding interaction. Upon the initial binding event of a single conjugated FA to the FBP, the FBP undergoes a conformational change[51,52] which exposes a more hydrophilic surface, enabling the irreversible van der Waals interaction with the polymer.

EXPERIMENTAL SECTION

Materials. All chemicals and materials were purchased from Sigma-Aldrich or Fischer Scientific and used as received unless otherwise specified. G5 PAMAM dendrimer was purchased from Dendritech and purified as previously reported to remove trailing generation and G5 oligomer impurities.[43] Cyclooct-1-yne-3-glycolic acid (COG) was synthesized from a modified literature preparation (see Supporting Information).[53] Synthesis and characterization of γ-azide-Lys-Asp-folic acid (γ-azide-FA) can be found in the Supporting Information.

Preparation of G5-Ac-$COG_{4.0(avg)}$ Conjugates. Conjugates were prepared from G5 dendrimer and COG via amide coupling. In brief, amine-terminated G5 (202.6 mg) was dissolved to 0.16 μM in DI water (45 mL). COG (4.9 mg) was activated by dissolving to 10.5 μM in acetonitrile (1.25 mL) with 2.65 equiv of 1-ethyl-3-(3-(dimethylamino)propyl)-carbodiimide (EDC) (14.0 mg) and 2.78 equiv of *N*-hydroxysuccinimide (NHS) (9.1 mg) and stirring for 2 h. The activated COG was added dropwise via syringe pump to the dendrimer solution and stirred overnight. The product was purified using Amicon Ultra Centrifugal units, 10 kDa cutoff membranes, with 2 phosphate buffered saline (PBS) washes and 4 deionized water (DI) washes. Product was isolated via lyophilization. The material (126.4 mg) was then fully

acetylated (converting 100% of the remaining primary amines to acetyl groups, henceforth designated "Ac") by redissolving in anhydrous methanol (0.19 μM, 24 mL) and adding 450 equiv of triethylamine (305 μL) and 360 equiv of acetic anhydride (166 μL), stirring for 4 h, purified by centrifugation, and isolated by lyophilization. G5-Ac-$COG_{4.0(avg)}$ (96.4 mg) was characterized by rp-UPLC.

Isolation of Precisely Defined G5-Ac-COG_x Conjugates. Dendrimers with precise ratios of COG ligands per dendrimer were isolated via rp-HPLC according to literature procedures.[48] Briefly, three 910 μL injections at a 32 mg/mL concentration of the averaged material were performed with a C18 column on a water/acetonitrile gradient with 0.1% TFA. Fractions were collected as the material eluted and combined to obtain samples with precisely x = 0−4 COG ligands per dendrimer. Products were purified using PD-10 desalting protocols, with DI as the equilibration buffer and samples dissolved in 10× PBS, then lyophilized to dry. Samples were characterized by rp-UPLC and ^{1}H NMR spectroscopy. Curve fitting of chromatograms by Igor Pro was performed to assess purity of precise ratio materials and to determine the average number of COG ligands of stochastic materials (Table S1 in the Supporting Information).

Synthesis of G5-Ac-FA_n Conjugates. Dendrimers with well-characterized numbers of covalently bound folic acids were synthesized via click reaction of G5-Ac-COG_x conjugates and γ-azide-FA. Briefly, 10 equiv of a stock γ-azide-FA solution (77 mM in DMSO) was added to dendrimer conjugates. The resulting mixtures were then brought to a final dendrimer concentration of approximately 310 μM to fully dissolve the dendrimer conjugates (see Table S2 in the Supporting Information for exact amounts used in each reaction). Solutions were agitated for 48 h, then diluted to 2.5 mL with DI, and purified using PD-10 desalting columns, gravity protocols, followed by 16 rounds of dialysis against DI. The samples were then further purified by repeating the PD-10 desalting column using 10× PBS to dilute the sample, followed by 2 rounds of dialysis against 1× PBS and 4 rounds against DI. Recovered samples were characterized by ^{1}H NMR spectroscopy and rp-UPLC. Curve fitting of chromatograms provided yield, purity, and FA average and distribution species for G5−FA_n materials.

Methods. *High Performance Liquid Chromatography.* Isolation of G5-Ac-COG_x was achieved with previously published protocols.[48]

LC Peak Fitting. Chromatograms were fit with Gaussian peaks using Igor Pro Version 6.0.3.1 software. Peak widths from chromatogram to chromatogram were kept constant.

Nuclear Magnetic Resonance Spectroscopy. NMR spectroscopy experiments were performed on a Varian MR400 instrument. ^{1}H NMR spectra were obtained used 10 s preacquisition delays and a total of 64 scans. All sample solutions were set to a dendrimer concentration of 1−5 mg/mL in deuterium oxide.

Surface Plasmon Resonance Spectroscopy. CM5 sensor chips were purchased for use in SPR experiments from GE Healthcare Life Sciences. SPR experiments were conducted in a Biacore X instrument (Pharmacia Biosensor AB). Two immobilized folate binding protein (FBP) chips were prepared following the suggested protocols: a solution of 0.2 M EDC and 0.05 M NHS was used as an activating solution, an immobilization solution of FBP at 1 mg/mL for the "low density" chip and 1.5 mg/mL for the "high density" chip, with ethanolamine as the deactivation solution. The surface density of FBP was approximately 10 and 20 ng/mm^2 for the low and high density chips, respectively. Flow cell two was employed as a control cell by activating and deactivating the surface without the addition of protein. The chips were characterized using free FA solutions and checked for nonspecific binding with a control of G5-Ac containing no COG or FA. Immobilization and free FA chromatograms can be found in the Supporting Information. The "high density" chip contains roughly double the amount of immobilized FBP according to total change in response units. Conjugate samples were dissolved in fresh HBS-EP buffer at 100 μM and serially diluted to 20, 10, 5, 2.5, and 1.25 μM in HBS-EP buffer from Fischer Scientific. Runs were multichannel, FC1-FC2, at 10 μL/min. The system was allowed to equilibrate at the beginning of each run for no less than 300 s, followed by a 2 min, 30 μL (50−5−5−5 bubble method) injection. The system was monitored for no less than 500 s postinjection. Between each run, the chip was washed with a 5 μL injection of pH 1.5 buffer to remove bound materials followed by an instrument prime step. The sensograms represent a subtraction of FC2 (no protein) from FC1 (protein immobilized).

RESULTS

Preparation of G5-Ac-$COG_{4.0(avg)}$ Conjugates (Figure 3a). 96.4 mg of G5-Ac-COG conjugate was prepared with an average of 4.0 COGs per dendrimer as calculated by rp-UPLC peak fitting (overall yield 41%). All samples were characterized by ^{1}H NMR spectroscopy (Figure S1 in the Supporting Information) and rp-UPLC.

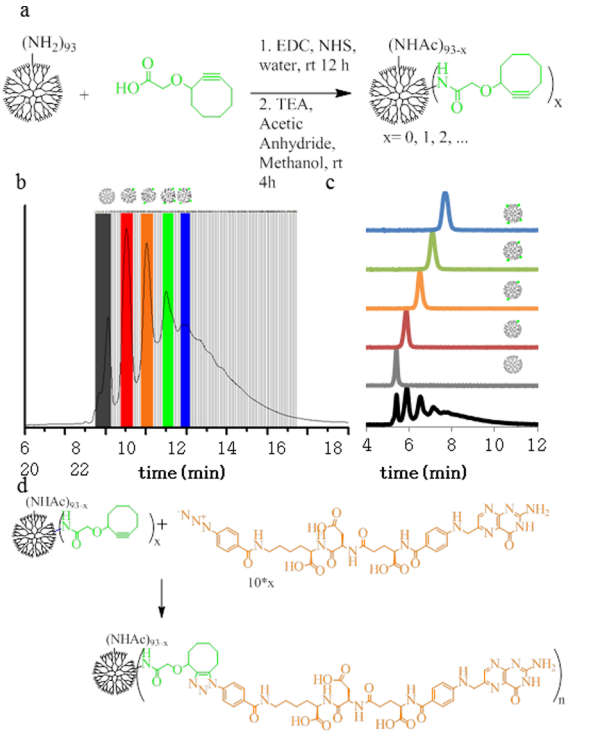

Figure 3. (a) Synthesis of PAMAM-COG conjugate. (b) Semiprep rp-HPLC isolation of PAMAM with 1, 2, 3, 4, or 5 COGs. (c) Isolated samples elute from rp-UPLC as a function of ligand-to-dendrimer ratio. (d) Scheme of G5-COG click reaction of γ-azide-FA.

Isolation of G5-Ac-COG_x Conjugates with Precise COG-to-Dendrimer Ratios (Figure 3b,c). Dendrimer

dx.doi.org/10.1021/mp5000967 | Mol. Pharmaceutics 2014, 11, 1696−1706

samples with x = 0−4 were isolated in quantities ranging from 3 to 8 mg. All samples were characterized by ^{1}H NMR spectroscopy (Figure S2 in the Supporting Information) and rp-UPLC (Table S1 in the Supporting Information).

Synthesis of G5-Ac-FA$_n$ Conjugates (Figure 3d). One equivalent of G5-Ac-COG$_x$ and 10x (x = 1−4) equivalents of γ-azide-FA were dissolved to give a dendrimer concentration of 310 μM in DMSO. Reaction mixtures were shaken for 48 h with occasional vortexing. Samples were then desalted according to the manufacturer's gravity protocol with PD-10 desalting columns (equilibration buffer as DI, sample dissolved in 10× PBS), and then dialyzed against DI using 10 000 Da cutoff membranes (16 media changes). Large amounts of unreacted γ-azide-FA remained after initial purification as detected by rp-UPLC. Two additional rounds of dialysis against 1× PBS buffer followed by 4 rounds against DI removed unreacted γ-azide-FA as assessed by rp-UPLC. Samples were characterized by rp-UPLC (Figure S3 in the Supporting Information) and ^{1}H NMR spectroscopy (Figure S4 in the Supporting Information). The n = 1 click reaction had an efficiency of 96%, while all other efficiencies ranged from 54 to 64% with mass recoveries over 95%. A detailed analysis of each sample's fractional composition is summarized in Table S3 in the Supporting Information. For these materials, HPLC provides the most accurate method for determining conjugate dendrimer ratios[54] (*vide infra* and Supporting Information) and % FA values are calculated on the basis of HPLC data.

Surface Plasmon Resonance Spectroscopy. Sensorgrams for G5-Ac-FA$_n$ (n = 0, 1.0, 1.2, 1.9, 2.7) were collected for both the low (Figure 4) and high (Figure 5) density chips. The unfunctionalized, neutral conjugate (n = 0) showed no specific binding at either chip density across all concentrations tested. All G5−FA conjugates showed specific binding to the FBP immobilized flow cell 1, which increased in a FA concentration dependent manner. After injection completion,

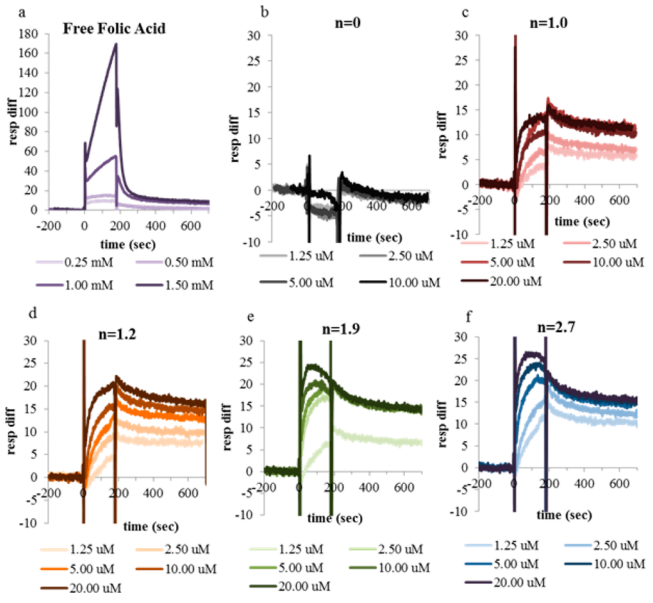

Figure 4. SPR sensograms of conjugates (n = 1.0, red; n = 1.2, orange; n = 1.9, green; n = 2.7, blue) and controls (n = 0, gray; free FA, purple) on lower density chip. The color gradient represents concentration from low (light) to high (dark). Free FA samples were run at millimolar as opposed to micromolar concentrations to obtain adequate signal.

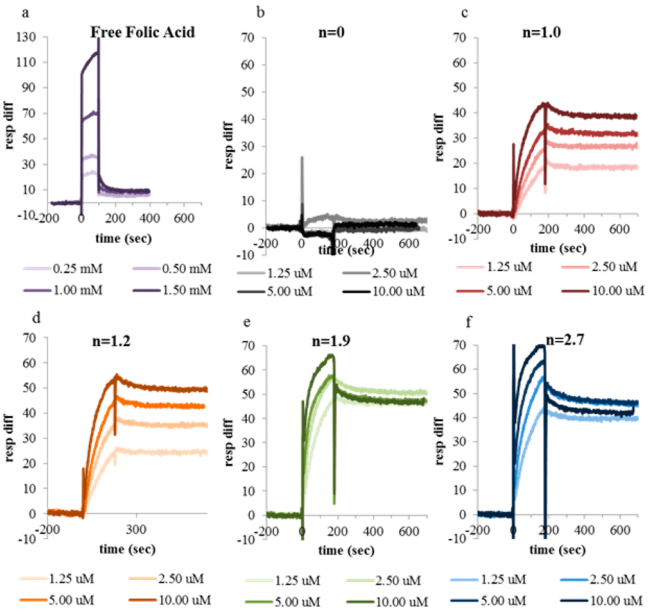

Figure 5. SPR sensograms of conjugates (n = 1.0, red; n = 1.2, orange; n = 1.9, green; n = 2.7, blue) and controls (n = 0, gray; free FA, purple) on higher density chip. The color gradient represents concentration from low (light) to high (dark).

all FA conjugated samples had a release profile. The association and dissociation phases were fit with various models for evaluation of k_a, k_d, and K_d.

DISCUSSION

rp-HPLC is an effective tool for isolating dendrimers with precise numbers of clickable ligands.[46,47] To date, four unique click ligands have been employed using the same gradient, with functional groups of azide,[47,48] alkyne,[46] a fluorinated ring strain promoted ligand,[48,54] and the cyclooctyne ligand presented here for the first time. This robust methodology allows isolation of various species containing single ligand/dendrimer ratios from heterogeneous, averaged samples containing 10 or more species. Due to the flexible nature of the PAMAM dendrimer and transient interaction of the ligand with the hydrophobic column, this technique has proven to be nonspecific to the relative location of the multiple ligands conjugated to the same sample, i.e., all dendrimer conjugated to three ligands coelutes, simplifying the separation process. Isolation of the G5-Ac-COG$_x$ conjugates utilized in this paper reflect the success of prior studies with other click ligands. All isolated samples of G5-Ac-COG$_x$ had single species purities over 95%. In the average sample, the most common species was dendrimer conjugated to 2 COG ligands, and this portion comprised only 16% of the sample. However, the isolated sample labeled G5-Ac-COG$_2$ contained only G5 conjugated to 2 ligands as measured by rp-UPLC, with no detectable presence of dendrimer conjugated to 0, 1, 3, or other numbers of ligands.

Here, we present the first application of the G5 PAMAM precise ligand-to-dendrimer ratio materials to a multivalent targeting system. FBP, employed as a model for the FAR overexpressed in various cancer cell lines, and the interaction of this target with FA has been a highly studied system for both cancer cell targeting of chemotherapeutics and for the more basic understanding of multivalent nanoparticle interactions. To understand how multivalency affects nanoparticle−ligand conjugate behavior in biological systems, it is vital to compare

dx.doi.org/10.1021/mp5000967 | *Mol. Pharmaceutics* 2014, 11, 1696−1706

monovalent particles to those with 2 or more targeting ligands. However, stochastically synthesized conjugates contain a distribution of ligands per particle, making it difficult to distinguish the behaviors of the individual populations. The controlled ligand/dendrimer ratio conjugates allowed for the synthesis of functional G5−FA_n materials with well-defined subpopulations, including a conjugate with a FA-to-dendrimer ratio of 1, with no higher valencies present. These materials, when studied by SPR, allowed comparison of the binding strength and potential for multivalent interaction of conjugates containing no more than 1, 2, 3, or 4 FA ligands (Table S3 in the Supporting Information).

Reaction of the COG conjugates with precise ligand-to-dendrimer ratios with complementary click functionalized FA allows for the generation of dendrimers with well-defined numbers of covalently conjugated FAs via orthogonal click chemistry between the ring-strained cyclooctyne on the dendrimer and an azido group on the modified FA. The reaction between G5-Ac-COG_1 and γ-azide-FA yielded a product that has 96% conjugate with a FA-to-dendrimer ratio of precisely 1 and 4% of a conjugate with no FA. Because the original sample had no dendrimer conjugated to 2 or more COG ligands, the resulting product has no material with the ability to undergo multivalent binding. This fact allows us to test both the Licata and Tkachenko key−lock/van der Waals interaction mechanism (Figure 2c),[45] which attributes the irreversible binding to dendrimer−protein van der Waals interactions and not multivalent FA binding, and the Sander mechanism[44] that assumes that monovalent behavior will significantly differ from bivalent and higher behavior. This critical piece of data would also have prevented the (incorrect) assessment by Banaszak Holl et al. that avidity increase is an exclusive function of conjugate valency.[31]

The remaining click reactions with the higher COG valent material went to about 60% completion despite a 10-fold excess of the γ-azide-FA. This result has been duplicated for G5−COG_x conjugates with this γ-azide-FA and other small molecules (unpublished data) within the lab, where reaction times greater than 48 h were tested. Similar reaction conditions employed in the literature between a G5-Ac-$COG_{\sim 20(avg)}$ conjugate and a γ-azide-modified methotrexate yielded 100% reaction efficiency, however in this case the limiting reagent was the small molecule.[53] This observation suggests that limiting the number of COG ligands on the dendrimer may limit accessibility for click reaction, perhaps via folding of hydrophobic ligands into the dendrimer core. The interior cavity of G5 PAMAM is limited, therefore with a high number (i.e., 20) of conjugated COG ligands, the dendrimer cannot internalize all the ligands at once, so at any given time COG ligands are available for conjugation. However, at lower numbers of COG ligands (i.e., 1−4 as described here) there is likely enough void volume in the dendrimer to hold all COG ligands at once, possibly preventing click reaction with solution species. Additionally, utilization of click chemistry with γ-azide-FA eliminates the less active α-FA that is bound through the α-carboxylic acid. Both structural isomers of the click reaction are likely present, although that alone would not be expected to have great effect on binding to the FBP. The presence of both isomers may contribute to peak broadening of the products in rp-UPLC (see Figure S3 in the Supporting Information). rp-UPLC also provides a useful tool for monitoring the click reaction, as the reaction of the hydrophobic ligand leads to a decrease in retention of the dendrimer conjugate on the C18 column. This technique provides a more accurate measurement of FA-to-dendrimer ratio of the product than techniques such as NMR, which only provides an average number and provides no detail about the individual ligand-to-dendrimer ratios that are present within a sample.[54] For this measurement the NMR spectroscopy based averages suffer from low signal for the conjugated species as compared to the polymer scaffold, and from the polydispersity of the scaffold employed (see Supporting Information).

Figure 6a compares the monovalent sample, G5-Ac-$FA_{1.0}$, to the Poisson distribution expected for a stochastically synthesized G5−FA conjugate with an average ratio of 1. By way of comparison, G5-Ac-$FA_{1.0}$ has only 4% unfunctionalized material compared to 37% in the stochastic material. More importantly, 26% of the stochastic material has two or more FAs covalently attached, meaning this material is not truly representative of monovalent behavior. The G5-Ac-$FA_{1.0}$ material may only undergo a single, monovalent specific interaction with a single FBP. Although the higher FA conjugates are not monodisperse, their heterogeneity has been significantly reduced as compared to an equivalent average stochastic conjugation. rp-UPLC has also revealed the relative amount of each ratio present in the samples (Figure 6b−d), allowing for a much better understanding of the contribution of each "*n*" valency species in the sample to the binding as a whole. For example, the product of the G5-Ac-COG_3 click reaction (G5-Ac-$FA_{1.9}$) has an average of ∼2 FAs per dendrimer, but UPLC reveals that 23% of the material has three FAs attached, while 49% has two FAs, 24% is monovalent, and 4% of the material has zero FA. The presence of dendrimer conjugated to more than 3 FAs is not possible as the starting material contained no dendrimer conjugated to 4 or more COGs. The equivalent stochastic average of n = 1.9 has significant concentrations of 10 unique FA-to-dendrimer ratios (ranging from 0 to ∼9), and ∼15% of the sample has zero FA.

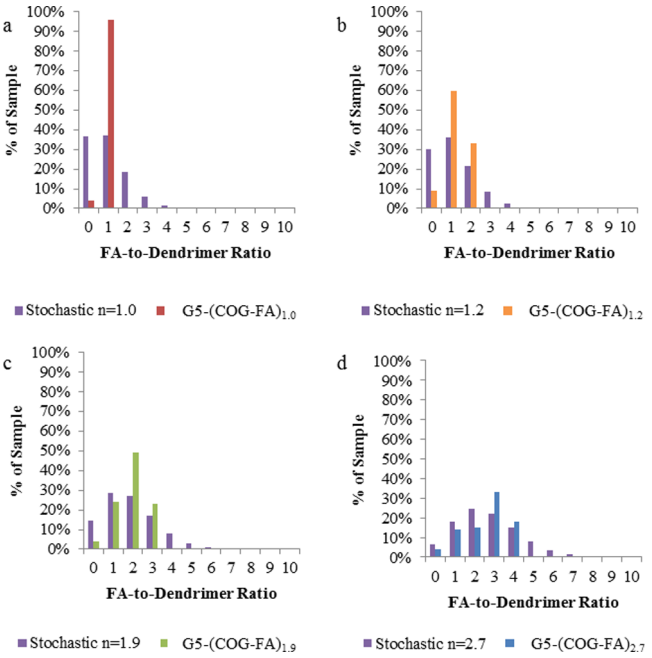

Figure 6. Comparison of distributions in click reaction products vs theoretical stochastically conjugated products (purple bars) of the same average for ratios of (a) 1.0 (red bars), (b) 1.2 (orange bars), (c) 1.9 (green bars), and (d) 2.7 (blue bars).

dx.doi.org/10.1021/mp5000967 | *Mol. Pharmaceutics* 2014, 11, 1696−1706

The decreased sample complexity and improved characterization for the samples summarized in Table S3 in the Supporting Information allow for more accurate interpretation of subsequent SPR results.

As illustrated in Figures 4 and 5, G5-Ac-FA_0 shows no binding to either of the FBP immobilized chips at the concentrations tested. However, G5−$FA_{n=1.0-2.7}$ have binding curves that saturate at higher concentration. The total signal during binding phase (0−200 s) (Figure 7) increases as a function of polymer concentration, FA valency (n), and density of protein immobilization.

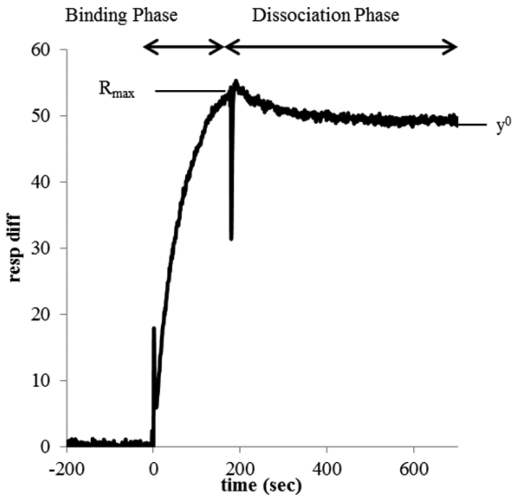

Figure 7. Definition of fitting parameters.

At 200 s, injection is complete and the dissociation phase begins (Figures 4 and 5). Several noteworthy observations can be made. First, at free FA concentrations ∼100-fold higher than the equivalent conjugated FA conditions, free FA returns to baseline in the low density chip and nearly to baseline in the high density chip. This observation is consistent with the expected, reversible binding of FA to FBP. G5-Ac-FA_0 also returns to baseline, indicating no irreversible interaction with the surface on the time scale of the experiment. Most importantly, monovalent G5-Ac-$FA_{1.0}$ has a significantly reduced dissociation rate as compared to FA (Figures 4c and 5c). In addition, G5-Ac-$FA_{1.0}$ does not return to baseline during the time scale of the experiment (500 s) at any concentration for either FBP surface density. The dissociation phase levels off substantially above the initial baseline, indicating that a portion of the material remains bound to the surface. This observation is true even though the highest relative FA concentration tested for G5-Ac-$FA_{1.0}$ (10 μM) is 25 times lower than the lowest FA concentration (0.25 mM). In other words, the dendrimer conjugate binds much more tightly than free FA (K_d ∼ 5−10 μM).

The irreversible binding on the time scale of the SPR experiment has previously been attributed to multivalent binding between the conjugate and receptor,[31,44] *however that cannot be the case for this purely monovalent conjugate*. This data strongly supports the key−lock/van der Waals binding mechanism proposed by Licata and Tkachenko[45] in which only one FA to FBP interaction is necessary to initiate the stronger interaction between the dendrimer and FBP, which itself is a result of the summation of many weak van der Waals interactions. This result contradicts the mechanism proposed by Sander et al.[44] that attributed all observed reversible binding to singly bound species. Hansen et al. have demonstrated using fluorescence spectroscopy that the tryptophan residues reorient upon folic acid binding to the FBP interior generating a more hydrophilic protein surface.[51,52] We hypothesize that this reorientation leads to the large increase in polymer−protein binding strength when FA is conjugated to the polymer.

More general observations can be made for the higher average conjugates. All G5-Ac-$FA_{n=1.0-2.7}$ have dissociation sensorgrams similar to those previously reported results on both the high and low density chips.[31] All samples have a portion of material that is irreversibly bound to the FBP surface on the time scale of this experiment (Figures 4 and 5). The saturation value ($y°$ value in Figure 7) changes as a function of FBP surface density (Figure 8). On the low density chip, the

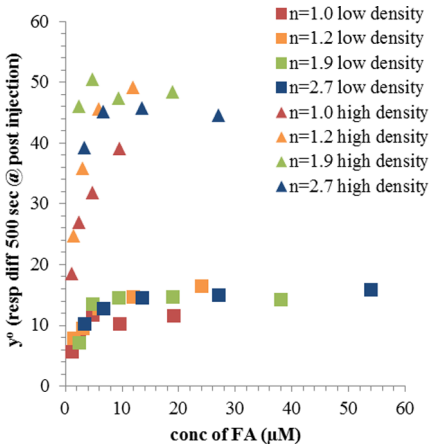

Figure 8. Saturation of irreversible bound material ($y°$) as a function of FA concentration.

maximum signal from irreversibly bound material is 14 ± 2 response units, which is achieved at a total FA solution concentration of ∼10 μM. On the high density surface, the response unit values saturate at 46 ± 4 at ∼10 μM. The only exception is G5-Ac-$FA_{1.0}$, for which 10 μM is the highest concentration tested. For both low and high FBP density, this conjugate did not reach the saturation value by 10 μM.

This surface density-dependent saturation of signal is indicative of a limiting number of FBP binding sites available for binding to the conjugates. Figure 8 also suggests that the total amount of irreversibly bound material is determined primarily by (i) total FA concentration in solution and (ii) surface FBP density. All differences in the irreversibly bound fraction for the multivalent (n = 1.2−2.7; orange, green, and blue) samples can be attributed to the difference in FA concentration of these samples, which completely saturates when total FA concentration is ∼10 μM. The monovalent material (G5-Ac-$FA_{1.0}$, red) appears to have slightly lower binding compared to the multivalent samples based on total FA concentration. This occurrence may result from the enhanced effective concentration in the multivalent samples due to dendritic architecture forcing the multiple FAs into a ∼5 diameter spherical area. This effect is small, and there appears to be no additional effect when valency is increased above n = 2. Qualitative observations (i.e., irreversible binding fraction in the G5-Ac-$FA_{1.0}$ sample and nonzero $y°$) indicate that this data will not adhere to the simple single phase Langmuir isotherm. To

dx.doi.org/10.1021/mp5000967 | *Mol. Pharmaceutics* 2014, 11, 1696−1706

demonstrate this relationship quantitatively, the data was fit with several models.

The development of the models and resulting fits may be found in the Supporting Information (Tables S4−S6, Figures S7 and S8). Several additional observations can be made. First, as expected, a single phase model (which mathematically describes Figure 2a) that assumes complete dissociation of the complex is a poor fit for the dissociation phase of all samples. The single phase *association* appears to have a good fit with the experimental data, however because this equation includes the single phase dissociation constant determined by the poorly fit dissociation phase, the overall mechanism is still invalid. Two phase dissociation fits the data significantly better for all valencies and concentrations. Second, the mathematical model equivalent to Figure 2b results in a poor fit for all the G5-Ac-$FA_{1.0}$ data. The two phase model (equivalent to the mechanism illustrated Figure 2c) had the best overall fit with an average residual of 2.39 response units. From this analysis, two main conclusions can be drawn: (1) There are at least two types (or steps) of association for G5−FA_n to the immobilized FBP, which leads to (2) the presence of both a transiently and irreversibly bound material for all G5−FA_n, including monovalent material. Clearly, in the original analysis of SPR data by Banaszak Holl et al.[31] (Figure 2a), the assumption that all bound material would eventually dissociate (i.e., $y' = 0$) from the surface was erroneous. The model proposed by Sander et al.[44] (Figure 2b) correctly noted that a fraction of the material remained bound to the surface for the length of the experiment (essentially irreversibly); however, the additional assumption that G5−FA_1, or G5−FA_n ($n \geq 1$) bound through a single FA/FBP bridge was entirely responsible for the observed dissociation in stochastic mixtures of G5−FA_n was incorrect. This model is clearly contradicted by the G5-Ac-$FA_{1.0}$ results, which are poorly fit by the equivalent mathematical model, and which clearly show enhanced binding to the FBP over free FA. When the other samples were fit with the same model, allowing for $n = 0$ or $n = 0$ and 1 to reversibly bind and $n \geq 2$ to irreversibly bind, poor association phase fits were observed (especially at lower FBP densities). The third theory, put forth by Licata and Tkachenko,[45] proposed that an initial binding event between conjugate and FBP is keyed by FA, and then the binding strength becomes dominated by van der Waals forces between the ∼30 kDa polymer and ∼40 kDa protein (Figure 2c). These summed weak interactions are responsible for the increased avidity for the conjugates, which the authors hypothesized are too great to be attributed to the comparatively weak (K_d ∼ 5−10 μM) FA/FBP interaction. Mathematically, this model would not show a dependence of K_d on degree of FA valency and is best represented schematically in Figure 2c (and quantitatively by eq 6 in the Supporting Information), which allows all conjugates with at least one FA to undergo both transient (FA/FBP bridge formation) and irreversible (formation of a strong complex between the PAMAM and FBP) binding events. The increased avidity for the G5-Ac-$FA_{1.0}$ conjugate as compared to free FA on both the low and high surface density chips, which is not further improved even with the G5-Ac-$FA_{2.7}$ conjugate, best agrees with this model qualitatively and quantitatively.

Therefore, we propose that the binding between G5-Ac-FA_n conjugates and immobilized FBP can be explained by a 2-fold mechanism. First, G5-Ac-FA_n binds to a FBP immobilized on the chip surface. This interaction has an association constant (k_{a2}) of ∼14 nM^{-1} s^{-1}. Because the initial binding is dependent on the concentration of FA, there is an enhancement of avidity due to an increased total concentration of FA when multiple copies of the ligand are attached to the same dendrimer. This effective concentration may also lead to an increased chance of rebinding, as the FA/FBP dissociation constant (k_{d2}) of ∼9 s^{-1} allows for dissociation of the conjugate from the surface on the SPR experimental time scale. Therefore, although strong binding is observed for all samples, the G5-Ac-$FA_{1.0}$ binds slightly less total material at the same relative FA concentration as compared to higher valency samples. After the FA binds to the FBP, the protein undergoes a conformational change,[51,52] exposing a more hydrophilic surface. In the second step, the acetylated dendrimer arms, which are in close proximity to the protein because of the initial FA−FBP key−lock interaction, interact via van der Waals forces with the FBP. We hypothesize that the interaction is further energetically driven by the rearrangement of FBP to yield a more hydrophilic surface after FA binding.[51,52] Although individual van der Waals interactions are weak, the sum of many interactions available between the two ∼5 nm entities and the associated desolvation create a force that is irreversible over the time scale of these SPR experiments.

Similar hydrophobic interactions are known to significantly contribute to the interactions between two proteins.[55,56] Experimental and theoretical measurements indicate that van der Waals interactions are effective only over a very short range (1−2 Å),[56] which supports the need for the FA/FBP interaction to key the hydrophobic interaction. Additionally, it has been observed that flexibility in at least one interacting protein strongly enhances the ability for van der Waals interactions to occur between proteins.[57−59] As PAMAM dendrimers are known to be highly flexible, these observations also support the hypothesis of nonspecific interaction between the polymer and protein surface.

The model proposed here is related to the well-known case of slow, tight binding previously described in detail for enzyme inhibitors.[49,50,60] Indeed, this behavior has been observed for folate analogues interacting with dihydrofolate reductase.[61] For the case of the FA−PAMAM conjugates, the rapid FA−FBP equilibrium is followed by the irreversible PAMAM−FBP binding to form a tight, stable complex. As illustrated in Figure 2c, the PAMAM dendrimer is believed to rearrange to allow the van der Waals interactions with the protein. Additionally, it is likely that a rearrangement of the FBP upon binding to the conjugated FA exposes a more hydrophilic surface,[51,52] enabling this interaction only when at least one FA is conjugated to the PAMAM.

■ CONCLUSIONS

In summary, we have synthesized a monovalent G5-Ac-$FA_{1.0}$ conjugate that allows for the distinction between three previously proposed mechanisms for the high avidity interaction with FBP. We have also synthesized multivalent G5−FA conjugates with narrow, nonstochastic FA-to-dendrimer ratio distributions to examine the kinetics of interaction between dendrimer-conjugated FA and FBP. The removal of trailing generations and oligomers in the PAMAM dendrimer starting material enabled the decoupling of mass and polymer surface area effects from FA valency. rp-HPLC enabled the isolation of dendrimers containing precise ratios (1, 2, 3, and 4) of copper-free, ring strain promoted click ligands to a dendrimer scaffold. A γ-azide-FA was clicked to these precise ratio conjugates to synthesize FA functionalized dendrimers

dx.doi.org/10.1021/mp5000967 | *Mol. Pharmaceutics* 2014, 11, 1696−1706

with narrow, well-defined distributions of FA with average ratios of up to 2.7 FAs per dendrimer. Importantly, the monovalent conjugate G5-Ac-$FA_{1.0}$ was synthesized with no portion of the sample having more than 1 conjugated FA, allowing for the distinction of polymer contributions (i.e., solubility and van der Waals interactions with the surface) from multivalent contributions (i.e., effective concentration and chelate binding) to the increased binding of dendrimer conjugates to FBP surfaces. SPR studies revealed that G5-Ac-FA_1 experiences the enhanced avidity over free FA that has previously been attributed to multivalent FA binding. Through examination of four quantitative models, it was concluded that the mechanism of interaction between G5-Ac-FA_n and surface immobilized FBP is 2-fold: an initial, reversible, FA concentration dependent key−lock or slow-onset, tight-binding interaction between the conjugate and protein, followed by irreversible interaction between the dendrimer and protein surfaces. The confirmation that these samples, *even for a monovalent sample*, exhibit irreversible binding on the time scale of the FA experiment disproves the original interpretation of Banaszak Holl et al.[31] These findings also provide evidence against the model proposed by Sander et al.,[44] which attributed the increase in avidity to dendrimer species with 2 or more conjugated FAs and assigned all dissociated material as singly bound. However, the model proposed by Licata et al.[45] explains the original data[31] and agrees well with these new findings. This van der Waals interaction model is in agreement with similar observations between two proteins in the literature[59] and consistent the reported rearrangement of FBP structure following FA binding.[51,52]

The mechanism proposed here is based on SPR experiments with an immobilized FBP on a three-dimensional surface. By way of contrast, cellular uptake mechanisms for FA targeted entities involve binding to FAR on a fluctuating cell membrane. The data and conclusions are directly comparable to previous studies that employed this model system; however, the results only serve to provide a possible hypothesis for the interaction mechanism of folate−polymer conjugates with cell-membrane bound FAR. The interaction of G5-Ac-FITC-FA_n with folic acid receptor upregulated KB cells, reported along with the original SPR experiments,[31] exhibited the same saturation behavior as a function of ligand number (n). Based on the data and mechanistic interpretation presented here and in the work of Licata and Tkachenko,[45] the observed enhancement of residence on the KB cell surface as a function of n could result from a combination of overall increased FA concentration and increased rebinding with increasing n. Alternatively, it is possible that conjugate-initiated receptor clustering occurs on the cell membrane which is impossible for the FBP immobilized to a dextran surface. Experiments to synthesize fluorescent materials containing precise ratios of FA targeting ligand for cell culture and *in vivo* experiments are in progress.

■ ASSOCIATED CONTENT

Supporting Information

Additional details of synthesis and experimental results and development of mathematical models. This material is available free of charge via the Internet at http://pubs.acs.org.

■ AUTHOR INFORMATION

Corresponding Author

*E-mail: mbanasza@umich.edu.

Notes

The authors declare no competing financial interest.

■ ACKNOWLEDGMENTS

This work was supported in part with Federal funds from the National Cancer Institute, National Institutes of Health, under Award RO1 CA119409.

■ REFERENCES

(1) Leamon, C. Folate-targeted chemotherapy. *Adv. Drug Delivery Rev.* **2004**, *56* (8), 1127−1141.
(2) Hilgenbrink, A. R.; Low, P. S. Folate receptor-mediated drug targeting: From therapeutics to diagnostics. *J. Pharm. Sci.* **2005**, *94* (10), 2135−2146.
(3) Paulos, C. Folate receptor-mediated targeting of therapeutic and imaging agents to activated macrophages in rheumatoid arthritis. *Adv. Drug Delivery Rev.* **2004**, *56* (8), 1205−1217.
(4) York, A. W.; Zhang, Y.; Holley, A. C.; Guo, Y.; Huang, F.; McCormick, C. L. Facile Synthesis of Multivalent Folate-Block Copolymer Conjugates via Aqueous RAFT Polymerization: Targeted Delivery of siRNA and Subsequent Gene Suppression. *Biomacromolecules* **2009**, *10* (4), 936−943.
(5) Liu, H.; Xu, Y.; Wen, S.; Chen, Q.; Zheng, L.; Shen, M.; Zhao, J.; Zhang, G.; Shi, X. Targeted Tumor Computed Tomography Imaging Using Low-Generation Dendrimer-Stabilized Gold Nanoparticles. *Chem.—Eur. J.* **2013**, *19* (20), 6409−6416.
(6) Low, P. S.; Henne, W. A.; Doorneweerd, D. D. Discovery and Development of Folic-Acid-Based Receptor Targeting for Imaging and Therapy of Cancer and Inflammatory Diseases. *Acc. Chem. Res.* **2007**, *41* (1), 120−129.
(7) Chen, C.; Jiyuan, K.; Zhou, X. E.; Wei, Y.; Joseph, S. B.; Jun, L.; Eu-Leong, Y.; Xu, H. E.; Karsten, M. Structural basis for molecular recognition of folic acid by folate receptors. *Nature* **2013**, *500* (7463), 486−489.
(8) Leamon, C. P.; Low, P. S. Delivery of macromolecules into living cells: a method that exploits folate receptor endocytosis. *Proc. Natl. Acad. Sci. U.S.A.* **1991**, *88* (13), 5572−5576.
(9) Kamen, B. A.; Capdevila, A. Receptor-mediated folate accumulation is regulated by the cellular folate content. *Proc. Natl. Acad. Sci. U.S.A.* **1986**, *83* (16), 5983−5987.
(10) Wang, Y.; Cao, X.; Guo, R.; Shen, M.; Zhang, M.; Zhu, M.; Shi, X. Targeted delivery of doxorubicin into cancer cells using a folic acid−dendrimer conjugate. *Polym. Chem.* **2011**, *2* (8), 1754.
(11) Zong, H.; Thomas, T. P.; Lee, K.-H.; Desai, A. M.; Li, M.-h.; Kotlyar, A.; Zhang, Y.; Leroueil, P. R.; Gam, J. J.; Banaszak Holl, M. M.; Baker, J. R. Bifunctional PAMAM Dendrimer Conjugates of Folic Acid and Methotrexate with Defined Ratio. *Biomacromolecules* **2012**, *13* (4), 982−991.
(12) Leamon, C. P.; Pastan, I.; Low, P. S. Cytotoxicity of folate-Pseudomonas exotoxin conjugates toward tumor cells. Contribution of translocation domain. *J. Biol. Chem.* **1993**, *268* (33), 24847−54.
(13) Liong, M.; Lu, J.; Kovochich, M.; Xia, T.; Ruehm, S. G.; Nel, A. E.; Tamanoi, F.; Zink, J. I. Multifunctional Inorganic Nanoparticles for Imaging, Targeting, and Drug Delivery. *ACS Nano* **2008**, *2* (5), 889−896.
(14) Shi, X.; Wang, S.; Meshinchi, S.; Van Antwerp, M. E.; Bi, X.; Lee, I.; Baker, J. R. Dendrimer-Entrapped Gold Nanoparticles as a Platform for Cancer-Cell Targeting and Imaging. *Small* **2007**, *3* (7), 1245−1252.
(15) Lu, Y.; Sega, E.; Leamon, C. P.; Low, P. S. Folate receptor-targeted immunotherapy of cancer: mechanism and therapeutic potential. *Adv. Drug Delivery Rev.* **2004**, *56* (8), 1161−1176.
(16) Gabizon, A.; Horowitz, A. T.; Goren, D.; Tzemach, D.; Mandelbaum-Shavit, F.; Qazen, M. M.; Zalipsky, S. Targeting Folate Receptor with Folate Linked to Extremities of Poly(ethylene glycol)-Grafted Liposomes: In Vitro Studies. *Bioconjugate Chem.* **1999**, *10* (2), 289−298.

(17) Kukowska-Latallo, J. F.; Candido, K. A.; Cao, Z.; Nigavekar, S. S.; Majoros, I. J.; Thomas, T. P.; Balogh, L. P.; Khan, M. K.; Baker, J. R. Nanoparticle Targeting of Anticancer Drug Improves Therapeutic Response in Animal Model of Human Epithelial Cancer. *Cancer Res.* **2005**, *65* (12), 5317−5324.
(18) Majoros, I. J.; Myc, A.; Thomas, T.; Mehta, C. B.; Baker, J. R. PAMAM Dendrimer-Based Multifunctional Conjugate for Cancer Therapy: Synthesis, Characterization, and Functionality. *Biomacromolecules* **2006**, *7* (2), 572−579.
(19) Quintana, A.; Raczka, E.; Piehler, L.; Lee, I.; Myc, A.; Majoros, I.; Patri, A.; Thomas, T.; Mulé, J.; Baker, J., Jr. Design and Function of a Dendrimer-Based Therapeutic Nanodevice Targeted to Tumor Cells Through the Folate Receptor. *Pharm. Res.* **2002**, *19* (9), 1310−1316.
(20) Djohari, H.; Dormidontova, E. E. Kinetics of Nanoparticle Targeting by Dissipative Particle Dynamics Simulations. *Biomacromolecules* **2009**, *10* (11), 3089−3097.
(21) Wang, S.; Dormidontova, E. E. Nanoparticle Design Optimization for Enhanced Targeting: Monte Carlo Simulations. *Biomacromolecules* **2010**, *11* (7), 1785−1795.
(22) Wang, S.; Dormidontova, E. E. Nanoparticle targeting using multivalent ligands: computer modeling. *Soft Matter* **2011**, *7* (9), 4435−4445.
(23) Martinez-Veracoechea, F. J.; Frenkel, D. Designing super selectivity in multivalent nano-particle binding. *Proc. Natl. Acad. Sci. U.S.A.* **2011**, *108* (27), 10963−10968.
(24) Kitov, P. I.; Bundle, D. R. On the Nature of the Multivalency Effect: A Thermodynamic Model. *J. Am. Chem. Soc.* **2003**, *125* (52), 16271−16284.
(25) Krishnamurthy, V. M.; Estroff, L. A.; Whitesides, G. M. Multivalency in Ligand Design. In *Fragment-based Approaches in Drug Discovery*; Wiley-VCH Verlag GmbH & Co. KGaA: 2006; pp 11−53.
(26) Wolfenden, M. L.; Cloninger, M. J. Multivalency in Carbohydrate Binding. In *Carbohydrate Recognition*; John Wiley & Sons, Inc.: 2011; pp 349−370.
(27) Chittasupho, C. Multivalent ligand: design principle for targeted therapeutic delivery approach. *Ther. Delivery* **2012**, *3* (10), 1171−1187.
(28) Kiessling, L. L.; Gestwicki, J. E.; Strong, L. E. Synthetic multivalent ligands in the exploration of cell-surface interactions. *Curr. Opin. Chem. Biol.* **2000**, *4* (6), 696−703.
(29) Kiessling, L. L.; Strong, L. E.; Gestwicki, J. E. Principles for multivalent ligand design. *Annu. Rep. Med. Chem.* **2000**, *35*, 321−330.
(30) Mullen, D. G.; Banaszak Holl, M. M. Heterogeneous Ligand−Nanoparticle Distributions: A Major Obstacle to Scientific Understanding and Commercial Translation. *Acc. Chem. Res.* **2011**, *44* (11), 1135−1145.
(31) Hong, S.; Leroueil, P. R.; Majoros, I. J.; Orr, B. G.; Baker, J. R.; Banaszak Holl, M. M. The Binding Avidity of a Nanoparticle-Based Multivalent Targeted Drug Delivery Platform. *Chem. Biol.* **2007**, *14* (1), 107−115.
(32) Kuroiwa, Y.; Takakusagi, Y.; Kusayanagi, T.; Kuramochi, K.; Imai, T.; Hirayama, T.; Ito, I.; Yoshida, M.; Sakaguchi, K.; Sugawara, F. Identification and Characterization of the Direct Interaction between Methotrexate (MTX) and High-Mobility Group Box 1 (HMGB1) Protein. *PLoS One* **2013**, *8* (5), e63073.
(33) Silpe, J. E.; Sumit, M.; Huang, B.; Kotlyar, A.; van Dongen, M. A.; Banaszak Holl, M. M.; Orr, B. G.; Choi, S. K. Avidity Modulation of Folate-Targeted Multivalent Dendrimers for Evaluating Biophysical Models of Cancer Targeting Nanoparticles. *ACS Chem. Biol.* **2013**, *8*, 2063−2071.
(34) Zhang, Y.; Thomas, T. P.; Lee, K.-H.; Li, M.; Zong, H.; Desai, A. M.; Kotlyar, A.; Huang, B.; Banaszak Holl, M. M.; Baker, J. R., Jr. Polyvalent saccharide-functionalized generation 3 poly(amidoamine) dendrimer−methotrexate conjugate as a potential anticancer agent. *Bioorg. Med. Chem.* **2011**, *19* (8), 2557−2564.
(35) Stella, B.; Arpicco, S.; Peracchia, M. T.; Desmaele, D.; Hoebeke, J.; Renoir, M.; D'angelo, J.; Cattel, L.; Couvreur, P. Design of Folic Acid-Conjugated Nanoparticles for Drug Targeting. *J. Pharm. Sci.* **2000**, *89* (11), 1452−1464.
(36) Wiener, E. C.; Konda, S.; Shadron, A.; Brechbiel, M.; Gansow, O. Targeting Dendrimer-Chelates to Tumors and Tumor Cells Expressing the High-Affinity Folate Receptor. *Invest. Radiol.* **1997**, *32* (12), 748−754.
(37) Patri, A.; Kukowskalatallo, J.; Baker, J. R., Jr. Targeted drug delivery with dendrimers: Comparison of the release kinetics of covalently conjugated drug and non-covalent drug inclusion complex. *Adv. Drug Delivery Rev.* **2005**, *57* (15), 2203−2214.
(38) Mintzer, M. A.; Grinstaff, M. W. Biomedical applications of dendrimers: a tutorial. *Chem. Soc. Rev.* **2011**, *40* (1), 173−190.
(39) Christensen, J. B.; Tomalia, D. A. Designing Dendrimers. In *Dendrimers as Quantized Nano-modules in the Nanotechnology Field*; Campagna, S., Ceroni, P., Puntoriero, F., Eds.; J. Wiley & Sons: Hoboken, 2012; pp 1−33.
(40) Tomalia, D. A.; Christensen, J. B.; Boas, U. The Dendritic State. *Dendrimers, Dendrons Dendritic Polym.* **2012**, 2−32.
(41) Tomalia, D. A.; Huang, B.; Swanson, D. R.; Brothers, H. M.; Klimash, J. W. Structure control within poly(amidoamine) dendrimers: size, shape and regio-chemical mimicry of globular proteins. *Tetrahedron* **2003**, *59*, 379−3813.
(42) Chauhan, A. S.; Jain, N. K.; Diwan, P. V. Pre-clinical and behavioural toxicity profile of PAMAM dendrimers in mice. *Proc. R. Soc. A* **2010**, *466* (2117), 1535−1550.
(43) van Dongen, M. A.; Desai, A.; Orr, B. G.; Baker, J. R., Jr.; Banaszak Holl, M. M. Quantitative analysis of generation and branch defects in G5 poly(amidoamine) dendrimer. *Polymer* **2013**, *54*, 4126−4133.
(44) Waddell, J. N.; Mullen, D. G.; Orr, B. G.; Banaszak Holl, M. M.; Sander, L. M. Origin of broad polydispersion in functionalized dendrimers and its effects on cancer-cell binding affinity. *Phys. Rev. E* **2010**, *82*, 036108.
(45) Licata, N. A.; Tkachenko, A. V. Kinetic Limitations of Cooperativity-Based Drug Delivery Systems. *Phys. Rev. Lett.* **2008**, *100*, 158102.
(46) Mullen, D. G.; Fang, M.; Desai, A.; Baker, J. R., Jr.; Orr, B. G.; Banaszak Holl, M. M. A Quantitative Assessment of Nanoparticle-Ligand Distributions: Implications for Targeted Drug and Imaging Delivery in Dendrimer Conjugates. *ACS Nano* **2010**, *4*, 657−670.
(47) Mullen, D. G.; Borgmeier, E. L.; Desai, A. M.; van Dongen, M. A.; Barash, M.; Cheng, X.-m.; Baker, J. R.; Banaszak Holl, M. M. Isolation and Characterization of Dendrimers with Precise Numbers of Functional Groups. *Chem.—Eur. J.* **2010**, *16* (35), 10675−10678.
(48) van Dongen, M. A.; Vaidyanathan, S.; Banaszak Holl, M. M. PAMAM Dendrimers as Quantized Building Blocks for Novel Nanostructures. *Soft Matter* **2013**, *9*, 11188−11196.
(49) Sculley, M. J.; Morrison, J. F. The determination of kinetic constants governing the slow,tight-binding inhibition of enzyme-catalysed reactions. *Biochim. Biophys. Acta, Protein Struct. Mol. Enzymol.* **1986**, *874* (1), 44−53.
(50) Sculley, M. J.; Morrison, J. F.; Cleland, W. W. Slow-binding inhibition: the general case. *Biochim. Biophys. Acta, Protein Struct. Mol. Enzymol.* **1996**, *1298* (1), 78−86.
(51) Bruun, S. W.; Holm, J.; Hansen, S. I.; Andersen, C. M.; Nørgaard, L. A Chemometric Analysis of Ligand-Induced Changes in Intrinsic Fluorescence of Folate Binding Protein Indicates a Link Between Altered Conformational Structure and Physico-Chemical Characteristics. *Appl. Spectrosc.* **2009**, *63* (12), 1315−1322.
(52) Holm, J.; Lawaetz, A. J.; Hansen, S. I. Ligand binding induces a sharp decrease in hydrophobicity of folate binding protein assessed by 1-anilinonaphthalene-8-sulphonate which suppresses self-association of the hydrophobic apo-protein. *Biochem. Biophys. Res. Commun.* **2012**, *425* (1), 19−24.
(53) Huang, B.; Desai, A.; Zong, H.; Tang, S.; Leroueil, P. R.; Baker, J. R., Jr. Copper-free click conjugation of methotrexate to a PAMAM dendrimer platfrom. *Tetrahedron Lett.* **2011**, *52*, 1411−1414.
(54) Dougherty, C. A.; Furgal, J. C.; van Dongen, M. A.; Goodson, T., III; Banaszak Holl, M. M.; Manono, J.; DiMaggio, S. Isolation and Characterization of Precise Dye/Dendrimer Ratios. *Chem.—Eur. J.* **2014**, DOI: 10.1002/chem.201304854.

(55) Ross, P. D.; Subramanian, S. Thermodynamics of protein association reactions: forces contributing to stability. *Biochemistry* **1981**, *20* (11), 3096−3102.
(56) Van Oss, C. J.; Good, R. J.; Chaudhury, M. K. The role of van der Waals forces and hydrogen bonds in "hydrophobic interactions" between biopolymers and low energy surfaces. *J. Colloid Interface Sci.* **1986**, *111* (2), 378−390.
(57) Cardone, A.; Pant, H.; Hassan, S. A. Specific and Non-Specific Protein Association in Solution: Computation of Solvent Effects and Prediction of First-Encounter Modes for Efficient Configurational Bias Monte Carlo Simulations. *J. Phys. B* **2013**, *117* (41), 12360−12374.
(58) Roth, C. M.; Neal, B. L.; Lenhoff, A. M. Van der Waals interactions involving proteins. *Biophys. J.* **1996**, *70* (2), 977−987.
(59) Molnár, T.; Vörös, J.; Szeder, B.; Takáts, K.; Kardos, J.; Katona, G.; Gráf, L. Comparison of complexes formed by a crustacean and a vertebrate trypsin with bovine pancreatic trypsin inhibitor − the key to achieving extreme stability? *FEBS J.* **2013**, *280* (22), 5750−5763.
(60) Szedlacsek, S. E.; Duggleby, R. G.; Daniel, L. P. Kinetics of slow and tight-binding inhibitors. *Methods Enzymol.* **1995**, *249*, 144−180.
(61) Williams, J. W.; Duggleby, R. G.; Cutler, R.; Morrison, J. F. The inhibition of dihydrofolate reductase by folate analogues: Structural requirements for slow- and tight-binding inhibition. *Biochem. Pharmacol.* **1980**, *29* (4), 589−595.